CPIA-Pub-498-V1, 1988, pp. 185–197.
[6]Liu, T. K., Perng, H. C., Luh, S. P., and Liu, F., "Aluminum Agglomeration in AP/RDX/Al/HTPB Propellant Combustion," *Journal of Propulsion and Power*, Vol. 8, No. 6, 1992, pp. 1177–1184.
[7]Turns, S. R., Wong, S. C., and Ryba, E., "Combustion of Aluminum-Based Slurry Agglomerates," *Combustion Science and Technology*, Vol. 54, Nos. 1–6, 1987, pp. 299–318.
[8]Salita, M., "Survey of Recent Al_2O_3 Droplet Size Data in Solid Rocket Chambers, Nozzles, and Plumes," 31st JANNAF Combustion Meeting (Sunnyvale, CA), Oct. 1994.
[9]Hermsen, R. W., "Aluminum Combustion Efficiency in Solid Rocket Motors," AIAA Paper 81-0038, Jan. 1981.
[10]Laredo, D., McCrorie, J. D., II, Vaughn, J. K., and Netzer, D. W., "Motor and Plume Particle Size Measurements in Solid Propellant Micromotors," *Journal of Propulsion and Power*, Vol. 10, No. 3, 1994, pp. 410–418.

Shock-Tunnel Investigation of Hypervelocity Free Shear Layers in a Planar Duct

D. R. Buttsworth* and R. G. Morgan†
University of Queensland, Queensland 4072, Australia

Introduction

WHILE fully developed mixing layers provide a useful configuration for fundamental investigations of turbulent compressible mixing,[1] other configurations such as transverse orifice injection,[2] wall slot injection,[3] and central strut injection,[4] are important because they directly model certain features of scramjet combustor flowfields. In the present work, hypervelocity mixing was studied using a central strut injection model of a scramjet. The term hypervelocity is used to distinguish the current study (in which the maximum flow velocity was approximately 4.3 $km \cdot s^{-1}$) from earlier work[5] in which the maximum flow velocity was much lower (approximately 1.3 $km \cdot s^{-1}$). The free shear layers were not fully developed and the majority of the pitot pressure measurements were made after the two mixing layers (from either side of the strut injector) met on the centerline of the injected stream. The present investigation examines the development of compressible mixing in the presence of relatively large hypervelocity boundary layers. This configuration differs significantly from the compressible mixing-layer configurations studied recently,[1,6] but is relevant because of the relatively high Reynolds number conditions anticipated in scramjet combustors.

Experiment

The T4 reflected shock tunnel and contoured hypersonic nozzle was operated at four different conditions with a nitrogen test gas. For the present experiments, disturbances that alter the nozzle reservoir pressure during the test time[7] were minimized through the appropriate selection of driver gas mixtures of helium and argon.[8] A planar duct that was 164 mm high and 80 mm wide was located centrally at the exit of the hypersonic nozzle (Fig. 1). A secondary stream from the base of a central strut was injected parallel to the shock tunnel (or primary) stream. The strut injector was 152 mm long and 7.59 mm high with an asymmetric 6.6-deg wedge at the leading edge. Inviscid calculations indicated that the asymmetric strut injector geometry should have a negligible effect on the flow conditions on either side of the strut injector.[8] The strut injector had a small contoured nozzle, which was designed (using the method of characteristics) to produce a uniform Mach 3 flow. The throat of the injection nozzle was 1.74 mm high, and the trailing edges were 0.19 mm thick. Hydrogen was supplied to the injector by a Ludwieg tube. Estimates of the primary and secondary stream conditions are given in Table 1 (additional details may be found in Ref. 8).

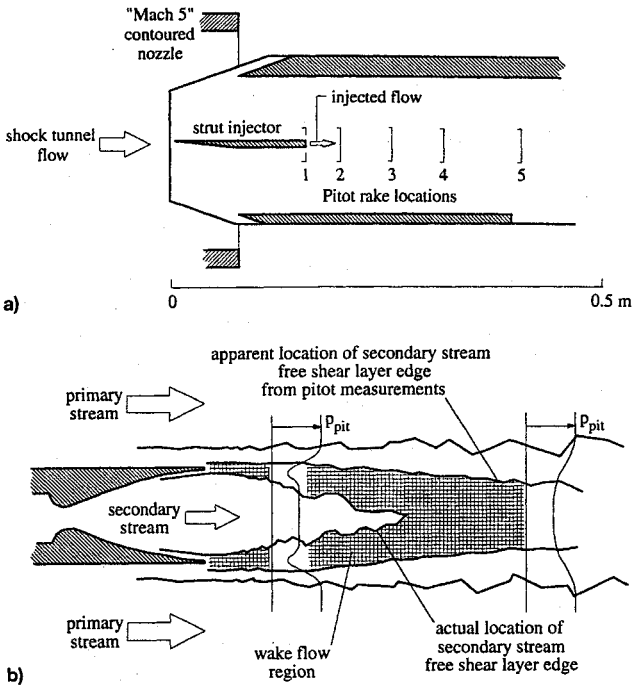

Fig. 1 Illustrations showing details of the planar duct model and the free shear-layer configuration. Stations 1–5 correspond to pitot rake measurements at x = 0, 40, 100, 160, and 250 mm: a) side view of the planar duct and b) schematic illustration of free shear-layer formation.

Pitot pressure measurements were obtained using piezoelectric transducers in a pitot rake with seven probes.[8] Each probe had an external diameter of 2.65 mm, an internal diameter of 2.04 mm, and an overall cavity length of approximately 27.5 mm. To determine the pressure indicative of the flow at the pitot rake location during the test time, a degree of averaging was necessary, because there was some acoustic resonance in the cavity ahead of the transducer. During the analysis of the pitot pressure signals, due caution was exercised to ensure that the results were influenced by neither the starting processes prior to the commencement of the useful test time, nor the slight decay in stagnation pressure, nor driver gas contamination that terminated the usable test flow.[8]

Results

Distributions of pitot pressure at five stations (see Fig. 1), corresponding to distances downstream from the injector trailing edge of 0, 40, 100, 160, and 250 mm, are presented in Fig. 2 for each of the operating conditions. At each station and condition, results are given for at least two shock-tunnel runs. (The pitot rake was offset vertically to improve the resolution of the measurements.)

The primary stream pitot pressure measured at station 2 was generally higher than at the other stations. Gun-tunnel experiments performed at similar Mach and Reynolds numbers with the same model demonstrated similar effects.[5] The increase in primary stream pitot pressure is attributed to the leading-edge shock waves from the duct side walls (because of boundary-

Received Oct. 27, 1995; revision received April 26, 1996; accepted for publication April 30, 1996.

*Postgraduate Student, Department of Mechanical Engineering; currently at the University of Oxford, Department of Engineering Science, Oxford, England, UK.
†Associate Professor, Department of Mechanical Engineering.

Table 1 Estimated primary and secondary stream parameters

Parameter	Condition 1	2	3	4
M_1	6.63	6.14	5.97	5.87
M_2	3.21	3.20	3.20	3.19
u_1, m·s^{-1}	2460	3300	3730	4280
u_2, m·s^{-1}	2400	2400	2400	2390
a_1, m·s^{-1}	371	537	625	729
a_2, m·s^{-1}	747	749	749	750
T_1, K	333	712	981	1350
T_2, K	96.7	97.1	97.1	97.5
p_1, kPa	7.75	10.0	11.3	12.2
p_2, kPa	4.03	4.49	5.66	6.94
ρ_1, kg·m^{-3}	0.0784	0.0473	0.0389	0.0304
ρ_2, kg·m^{-3}	0.0101	0.0112	0.0141	0.0173
Re_{u_1}, m^{-1}	9.99×10^6	4.80×10^6	3.66×10^6	2.73×10^6
Re_{u_2}, m^{-1}	5.84×10^6	6.45×10^6	8.13×10^6	9.93×10^6
γ_1	1.40	1.37	1.34	1.32
M_c	0.05	0.70	0.97	1.28

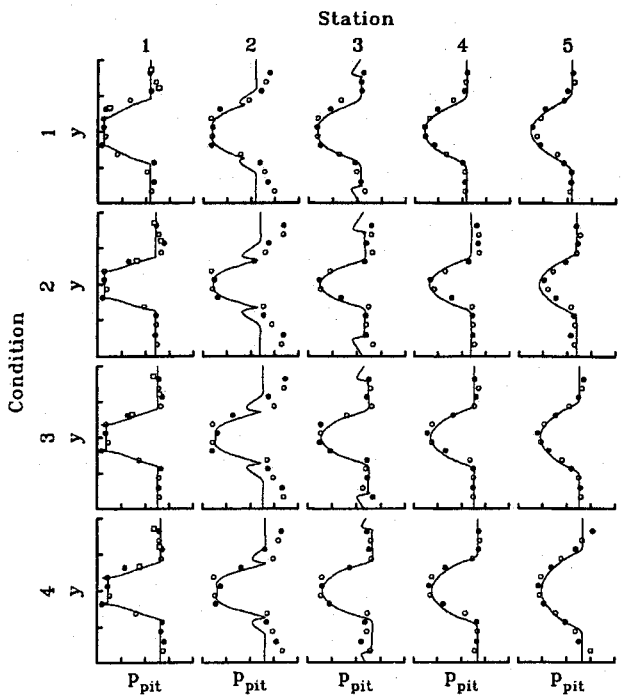

Fig. 2 Pitot pressure measurements. Each vertical division is 10 mm ($-20 < y < 20$ mm), and each horizontal division is 200 kPa ($0 < p_{pit} < 800$ kPa). Lines correspond to predictions obtained using the PNS code with the k-ε turbulence model.

layer growth), which arrive at the duct centerline downstream of station 1. Between stations 2 and 3, the primary stream pitot pressure relaxes to the undisturbed value as the leading-edge shock waves propagate away from the duct centerline.

It is known that the presence of shock waves can influence the mixing process.[9] Based on the maximum observed change in primary stream pitot pressure between stations 1 and 2, it is concluded that the present free shear layers were subjected to a shock wave system having an overall static pressure ratio of about 1.6. Preliminary estimates of the primary stream turbulence levels suggest that the rms velocity fluctuations were around 0.7% of the flow velocity.[10] Primary stream static pressure measurements across the width of the injector trailing edge were uniform to within approximately 10%.[8] A similar level of spanwise uniformity is anticipated for the secondary stream.

In Fig. 3, estimates of the apparent free shear-layer edges are presented. The edges were defined by a 5% change in pitot pressure as illustrated in Fig. 3a. At station 2, it was difficult to rigorously apply the pitot shear-layer edge definition to the experimental results. The error bars presented in Fig. 3 correspond to a distance of ±1 mm, which is thought to be a reasonable estimate incorporating the various uncertainties (including pitot-probe averaging and displacement effects) associated with the estimation of the 5% pitot edges.[8] It is important to note that these results do not locate the actual secondary stream edge of the free shear layer. This is because of the presence of a boundary-layer wake flow region as illustrated in Fig. 1b. Thus, the actual secondary stream shear-layer edge reached the centerline of the injected flow significantly earlier than is suggested by a cursory inspection of the results in Fig. 3.

The apparent thickness of the primary stream boundary layers at the injector trailing edge suggests that these boundary layers were turbulent. However, existing flat-plate data indicate that, for the present conditions, the boundary layers should be laminar.[10] It is therefore suggested that the disturbances that arise because of the sidewalls of the planar duct have a significant influence on transition process, as there were no side-walls on the measurement surface in the flat-plate experiments. Because of the low secondary stream Reynolds numbers at the exit of the injector nozzle (around 1.5×10^5), the secondary stream boundary layers were probably laminar. The thickness of the secondary stream boundary layers was estimated (using previous results[5,8]) to be 0.5 mm at the exit of the injector nozzle.

The pitot measurements (Fig. 2), and in particular, the spreading rate data (Fig. 3), appear to be largely independent of the convective Mach number M_c. Previous work has shown that the spreading rate of fully developed compressible mixing layers (prior to normalization with the incompressible estimate) can be independent of M_c, depending on the velocity and density ratios for the layer.[1] However, it is difficult to directly compare the present results with existing compressible mixing layer data because the present layers were far from a fully developed state (based on the criterion given in Ref. 6). The acceleration in growth of the primary stream shear-layer edge that occurs between stations 4 and 5 (see Fig. 3d), clearly demonstrates that the present free shear layers were not fully developed. In view of the developing state of the free shear layers, and because the results from conditions 2, 3, and 4 are largely similar to those obtained in the matched velocity case (condition 1), it appears reasonable to suppose that the large primary stream boundary layers on the strut injector had a strong influence on the mixing within the free shear layers in each case.

Parabolized Navier–Stokes (PNS) calculations of the free shear layers were performed using the code developed by Brescianini.[11] The PNS code uses the finite difference method of Patankar and Spalding[12] and calculates the pressure field using the SIMPLE algorithm.[13] Both the primary and secondary stream boundary layers were assumed to be fully turbulent at the injector trailing edge. As the free shear layers appeared to be symmetric about the centerline of the injected flow, only half

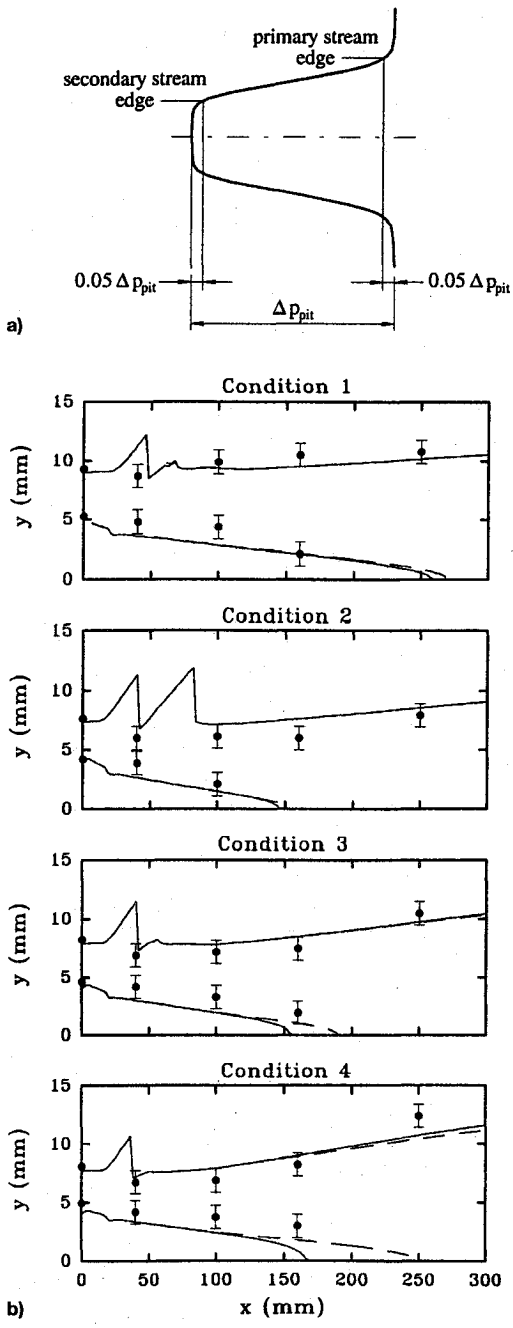

Fig. 3 Extent of free shear layers from pitot pressures. a) Definition of apparent shear-layer edges; b) experimental and theoretical results, solid lines (——) are results from the PNS code using the k-ε model, dashed lines (– – –) are results using the k-ε model with the compressibility correction, symbols are experimental results.

of the flowfield was modeled. The PNS code was implemented using a k-ε turbulence model[11,14] with the initial normalized length scale set to 0.03 for each mixing condition. (The initial normalized length scale equals the initial length scale divided by the initial shear region width, which in the present case was taken as the sum of the primary and secondary stream boundary-layer thicknesses.) The calculations used 500 grid points spread evenly from the centerline to a location approximately 60 mm above the centerline. This level of grid refinement was sufficient to ensure that the results were essentially grid independent.

The PNS predictions (Figs. 2 and 3) are generally in reasonable agreement with the experimental results. The discrepancies between the predictions and experimental results at station 2 are not unexpected because no attempt was made to model disturbances arising from the leading-edge shock waves caused by boundary-layer growth. The saw-tooth-like disturbances that are apparent in the theoretical results around this location are from waves generated by the initial static pressure difference between the two streams (Table 1), and therefore do not represent real variations in the shear-layer edge. Results obtained using the suggested compressibility correction[14] have also been plotted in Fig. 3. The correction took effect in the higher compressibility cases (conditions 3 and 4), but made only a relatively small difference. The PNS calculations did not predict the observed acceleration in the growth of the primary stream shear-layer edge.

Conclusions

Pitot pressure measurements were obtained in four different developing hypervelocity free shear layers. In general, the present results resemble those obtained in a previous study that was performed at significantly lower speeds, but at similar Reynolds number and Mach number conditions, and over a similar range of convective Mach numbers.[5] Although the interpretation of spreading rates is complicated slightly by the fact that the secondary stream was overexpanded, it appears the secondary stream was rapidly entrained into the free shear layer while there was very little spreading into the primary stream. There exists a high degree of similarity across the four mixing cases, including the case where the primary and secondary stream flow velocities were approximately matched. Thus, it appears probable that the relatively large primary stream boundary layers had a strong influence on these developing shear layers (particularly since a large fraction of the gas within the free shear layers came directly from the primary stream boundary layers). There was reasonable agreement between the experimental results and predictions made using a parabolized Navier–Stokes code with a k-ε turbulence model. However, a recently proposed k-ε compressibility correction that was validated for fully developed compressible mixing layers did not improve the predictions. Future investigations would benefit from additional data that assist in defining the initial free shear-layer conditions.

Acknowledgments

The authors wish to thank Craig Brescianini for allowing the use of his PNS code. We also wish to acknowledge the financial support of the Australian Research Council and NASA through NAGW-674.

References

[1]Papamoschou, D., and Roshko, A., "The Compressible Turbulent Shear Layer: An Experimental Study," *Journal of Fluid Mechanics*, Vol. 197, 1988, pp. 453–477.

[2]Bélanger, J., and Hornung, H. G., "Transverse Jet Mixing and Combustion Experiments in Hypervelocity Flows," *Journal of Propulsion and Power*, Vol. 12, No. 1, 1996, pp. 186–192.

[3]Kwok, K. T., Andrew, P. L., Ng, W. F., and Schetz, J. A., "Experimental Investigation of a Supersonic Shear Layer with Slot Injection of Helium," *AIAA Journal*, Vol. 29, No. 9, 1991, pp. 1426–1435.

[4]Casey R. T., and Stalker, R. J., "Hydrogen Mixing and Combustion in a High-Enthalpy Hypersonic Stream," *19th International Symposium on Shock Waves*, Vol. 1, Springer–Verlag, Berlin, 1995, pp. 151–156.

[5]Buttsworth, D. R., Morgan, R. G., and Jones, T. V., "A Gun Tunnel Investigation of Hypersonic Free Shear Layers in a Planar Duct," *Journal of Fluid Mechanics*, Vol. 299, 1995, pp. 133–152.

[6]Goebel, S. G., and Dutton, J. C., "Experimental Study of Compressible Turbulent Mixing Layers," *AIAA Journal*, Vol. 29, No. 4, 1991, pp. 538–546.

[7]Jacobs, P. A., Morgan, R. G., Stalker, R. J., and Mee, D. J., "Use of Argon-Helium Driver-Gas Mixtures in the T4 Shock Tunnel," *19th International Symposium on Shock Waves*, Vol. 1, Springer–Verlag, Berlin, 1995, pp. 263–268.

[8]Buttsworth, D. R., "Shock Induced Mixing and Combustion and in Scramjets," Ph.D. Dissertation, Dept. of Mechanical Engineering,

Univ. of Queensland, Australia, 1994.
[9]Shau, Y. R., and Dolling, D. S., "Exploratory Study of Turbulent Structure of a Compressible Shear Layer Using Fluctuating Pitot Pressure Measurements," *Experiments in Fluids*, Vol. 12, 1992, pp. 293–306.
[10]He, Y., and Morgan, R. G., "Transition of Compressible High Enthalpy Boundary Layer Flow over a Flat Plate," *Aeronautical Journal*, Vol. 98, No. 972, 1994, pp. 25–34.
[11]Brescianini, C. P., "An Investigation of the Wall-Injected Scramjet," Ph.D. Dissertation, Dept. of Mechanical Engineering, Univ. of Queensland, Australia, 1992.
[12]Patankar, S. V., and Spalding, D. B., *Heat and Mass Transfer in Boundary Layers*, 2nd ed., International Textbook, London, 1970.
[13]Elghobashi, S., and Spalding, D. B., "Equilibrium Chemical Reaction of Supersonic Hydrogen-Air Jets (The ALMA Computer Program)," NASA CR-2725, 1977.
[14]Brescianini, C. P., "Modified k-ε Model for Compressible Free Shear Flows," *AIAA Journal*, Vol. 30, No. 8, 1992, pp. 2161–2163.

Combustion of Liquid Oxygen with Hydrogen Under High-Pressure Conditions

An-Shik Yang*
National Space Program Office, Hsin-Chu 300, Taiwan, Republic of China
Wen H. Hsieh†
National Chung-Cheng University, Chia-Yi 621, Taiwan, Republic of China
and
Kenneth K. Kuo‡
Pennsylvania State University, University Park, Pennsylvania 16802

Introduction

LIQUID OXYGEN (LOX) and hydrogen have been used in various types of liquid rocket engines because of their high specific impulse and low exhaust pollution.[1] Numerous flow and chemical complexities involved in the LOX evaporation and combustion processes have attracted significant attention of many researchers.[2–11] Experiments have been carried out to determine the effects of important factors, such as droplet size, environmental pressure and temperature, and composition of the ambient gas on the combustion characteristics. Theoretical models have also been presented to elucidate the experimental observations and to predict the burning rate and/or lifetime of droplets. Since the fundamental study on the evaporation and chemical reaction processes of LOX in hydrogen-rich environments can be useful in advancing the knowledge of the overall spray combustion, the present work is motivated to explore the transport behavior and structure of a LOX/H_2 diffusion flame at elevated pressures.

Received July 28, 1995; revision received April 2, 1996; accepted for publication April 30, 1996.

*Staff Engineer, Mechanical Engineering Division. Member AIAA.
†Associate Professor, Graduate Institute of Mechanical Engineering. Member AIAA.
‡Distinguished Professor, Department of Mechanical Engineering. Fellow AIAA.

Experimental Apparatus

A gas-pressurized LOX feeding system was used to maintain a stable LOX surface at the exit of the feeding tube (6.35 mm diameter). The chamber pressure was maintained at a prespecified level by a computer feedback-controlled gas supply system. Instead of pure hydrogen, the mixture of helium and hydrogen was employed to pressurize the system for safety considerations. Another reason for using helium is because of its similar solubility features as hydrogen. Direct images of the flame shape of a LOX/hydrogen laminar diffusion flame were recorded using high-magnification video photography. For species concentration measurements, a quartz microprobe with an orifice diameter of 25 μm was used to sample the gas mixture in the postflame region. The gas mixture composition was analyzed using a Varian 3700 gas chromatograph (GC) with a thermal conductivity detector. Detailed description of the experimental setup can be found in Refs. 12 and 13.

Theoretical Approach

A theoretical model[12,13] was formulated to study combustion characteristics of LOX with the H_2/He mixture at elevated pressures. The physical model considers a column of LOX reacting with H_2/He mixture as shown in Fig. 1. Steady-state calculations were performed by considering the LOX being supplied at a certain feeding rate that kept its surface stationary. The gaseous oxygen and hydrogen react and form a stable diffusion flame anchored at the exit of the inner tube. It should be noted that the flame shape can be adjusted to accommodate a range of steady-state flow rates. The governing equations consist of a set of conservation equations of mass, momentum, energy, and species concentrations for a multicomponent system. To allow diffusion in the axial direction, the present analysis treats a fully elliptic problem. The gravitational body force was considered to account for the influence of natural convection. In the treatment of the real-gas behavior, pressure and temperature effects were included for evaluating thermodynamic and transport properties.[14–21] The flame-sheet approximation[22] with consideration of different mass diffusivities (i.e.,

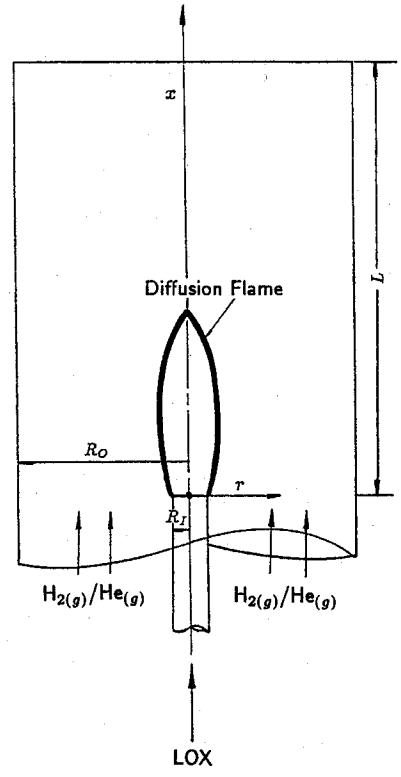

Fig. 1 Schematic diagram of the combustion of LOX with gaseous H_2/He mixture.